

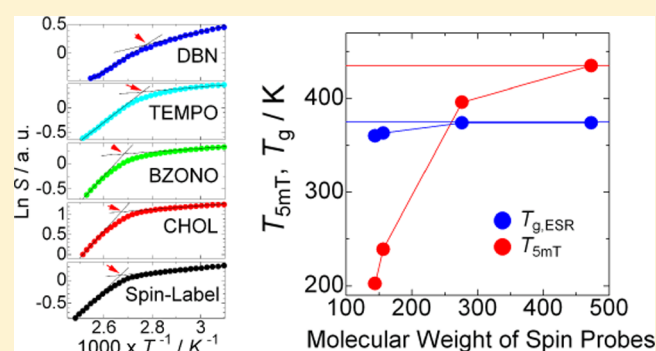
Simple and Highly Sensitive Measurement Method for Detection of Glass Transition Temperatures of Polymers: Application of ESR Power Saturation Phenomenon with Conventional Spin-Probe Technique

Yohei Miwa^{*,†} and Katsuhiro Yamamoto[‡]

[†]Department of Chemistry, Faculty of Engineering, Gifu University, Yanagido, Gifu 501-1193, Japan

[‡]Department of Materials Science and Technology, Nagoya Institute of Technology, Gokiso-cho, Showa-ku, Nagoya 466-8555, Japan

ABSTRACT: A combination of the microwave power saturation (MPS) method of electron spin resonance (ESR) and spin probing is proposed as a simple and practical technique for detecting the glass transition temperatures, T_g , of polymers with high sensitivity. Effects of the spin-probe size and concentration on the T_g value of polystyrene (PS) determined by MPS, $T_{g,ESR}$, were first evaluated. Spin-probed PS with four types of nitroxides, namely, di-*tert*-butyl nitroxide (DBN), 2,2,6,6-tetramethylpiperidine 1-oxyl (TEMPO), 4-benzoyloxy-2,2,6,6-tetramethylpiperidine-1-oxyl (BZONO), and 4',4'-dimethyl-spiro(5 α -cholestane-3,2'-oxazolidin)-3'-yloxy free radical (CHOL), having molecular weights of 144, 156, 276, and 473, respectively, and spin-labeled PS with TEMPO were prepared. The $T_{g,ESR}$ values for the spin-probed PS with DBN, TEMPO, BZONO, and CHOL and spin-labeled PS were determined to 360, 363, 374, 374, and 375 K, respectively, within experimental uncertainties of 2 K, whereas the glass transition temperature determined by DSC, $T_{g,DSC}$, was 375 K for all samples. A significant decrease in $T_{g,ESR}$ for small spin probes was shown to be due to decoupling between the mobilities of small spin probes and PS segments. Concerning the concentration, a decrease in the saturation factor, S , induced by shortening of the spin–spin relaxation time was observed for the spin-probed PS with CHOL when the concentration of CHOL was more than 1.0 wt %. Furthermore, $T_{g,ESR}$ decreased slightly with increasing weight fraction of CHOL because of the “plasticizer effect” of CHOL. However, the $T_{g,ESR}$ and $T_{g,DSC}$ values corresponded for each concentration. Thus, large spin probes, such as CHOL and BZONO, are appropriate for the determination of $T_{g,ESR}$ values; the concentration of the spin probes does not affect the $T_{g,ESR}$ value unless the overall T_g value is reduced by blending of excess spin probes. Finally, measurements of $T_{g,ESR}$ in PS/silica composites containing more than 95 wt % silica are shown as an application example of the present method. $T_{g,ESR}$ was clearly determined even for the PS/silica composites with 98 wt % silica; a decrease in $T_{g,ESR}$ with increasing silica content was observed.



1. INTRODUCTION

The glass transition is one of the most important physical phenomena for polymeric materials. Therefore, many measurements, such as differential scanning calorimetry (DSC), dilatometry, and dynamic mechanical analysis, have been applied to determine the glass transition temperature, T_g .¹ On the other hand, recent interest has been directed toward the T_g value in local regions and that of fractional components in inhomogeneous polymeric materials, such as polymer/inorganic or metal filler interfaces, immiscible polymer/polymer interfaces, free surfaces of polymer films, and polymers confined in small pores, because of both scientific interest and practical importance for designing high-performance materials such as nanocomposites, nanocoatings, and multilayer devices.² Generally speaking, selective determination of T_g in such local regions and for fractional components by conventional methods is difficult; however, several novel methods have

been developed and applied. For example, the T_g value at a film surface is efficiently determined by scanning probe microscopy, and a significant reduction of the T_g value at the film surface was discovered.^{3,4} Recently, Tanaka et al. reported an elevation of the T_g value at the interface of polystyrene (PS) with solid substrates by fluorescence lifetime measurements using evanescent wave excitation.^{5,6} On the other hand, Ellison and Torkelson developed a novel method to determine a local T_g value around fluorescence probes selectively from the temperature dependence of the emission intensity.⁷ They prepared a multilayer film on a silicon substrate consisting of pure and probe-dispersed polystyrene ultrathin films and successfully showed the distribution of the local T_g values from the free

Received: June 3, 2012

Revised: July 8, 2012

Published: July 9, 2012

surface to near the substrate. This technique was further applied to determine local T_g values in nanocomposites,^{8,9} block copolymers and multilayer films of different homopolymers,^{10,11} and nanopatterned polymers on silicon substrates.¹² As shown in these works, selective determination of the local T_g value using probe molecules is important and practical in polymer research.

Spin-label and spin-probe methods are traditional techniques for evaluating the mobility of soft matter through shape analysis of the electron spin resonance (ESR) spectra of paramagnetic molecules. Paramagnetic molecules are chemically bonded to target molecules in the spin-label method, whereas they are dispersed in the materials without chemical bonding in the spin-probe method.¹³ The spectral shape of the X-band ESR (ca. 9 GHz) is sensitive only on time scales in the range of 10^{-11} – 10^{-7} s;¹⁴ therefore, the determination of a T_g value is hard by this method because the change of the ESR spectral shape is small in the vicinity of T_g with a time scale of 100 s. On the other hand, some advanced ESR techniques can be applied to detect T_g values of soft materials. For example, Andreozzi et al. determined the temperature-dependent spin–lattice relaxation time, T_1 , of poly{[4-pentyloxy-3'-methyl-4'-(6-acryloxyxyloxy)]azobenzene} containing small amounts of the CHOL probe by longitudinally detected ESR.¹⁵ Sato et al. showed that the change in the temperature dependence of the T_1^{-1} value above and below the T_g value of glass-forming solvents (decalin, glycerol, 3-methylpentane, *o*-terphenyl, 1-propanol, sorbitol, sucrose, octacetane, and 1:1 water/glycerol) containing small amounts of nitroxides by the long-pulse saturation recovery technique.¹⁶ On the other hand, we recently developed a simple method, called the microwave power saturation (MPS) method, to determine the T_g values of spin-labeled polymers by monitoring the temperature dependence of the ESR signal intensity under an overloaded microwave power supply (typically more than 1 mW).^{17,18} This method allows the local T_g values of polymers to be measured around the spin-labeled sites with a very simple procedure using a common X-band ESR spectrometer without any equipment modifications. Moreover, limitations on the features of samples such as shape, color, and transparency are minimal for this measurement technique. This might be the most advantageous point of this technique compared to other modern optical methods.^{5–7}

In our previous work on the MPS method, nitroxides were chemically bonded to polymer chains to enhance the cooperativity between nitroxides and polymer segments.^{17,18} We used this technique to determine the local T_g values around the chain ends of poly(cyclohexyl acrylate) (PCHA) and polystyrene (PS).^{17,18} However, spin labeling is not easy and is impossible for some polymers. Preparing spin-probed polymers is much easier than preparing spin-labeled ones because nitroxides are merely dispersed in polymers without chemical bonding. However, which spin-probe reagent should be used? That is, does the molecular size of the spin probe affect the results? For example, in the case of the conventional shape analysis of ESR spectra, it is known that small spin probes move independently and that their mobility does not accurately reflect that of the polymer matrix.^{19,20} Moreover, what concentration of spin probes should be used? These topics are very important for practical use. Therefore, in the present work, we examined the effects of the spin-probe size and concentration on the T_g value of PS determined by the MPS method. Furthermore, as a practical example, the T_g values of

PS/silica composites containing more than 95 wt % silica were determined using the present method.

2. EXPERIMENTAL SECTION

2.1. Materials. Four types of nitroxides, namely, di-*tert*-butyl nitroxide (DBN), 2,2,6,6-tetramethylpiperidine 1-oxyl (TEMPO), 4-benzoyloxy-2,2,6,6-tetramethylpiperidine-1-oxyl (BZONO), and 4',4'-dimethyl-spiro(5 α -cholestane-3,2'-oxazolidin)-3'-yloxy free radical (CHOL), were purchased from Aldrich and used as received. The molecular weights of DBN, TEMPO, BZONO, and CHOL are 144, 156, 276, and 473, respectively. Nonporous silica powder (ADMAFINE, reported average diameter of 2 μ m) was obtained from Admatechs and dried at 423 K overnight in a vacuum.

2.2. Spin Labeling. PS was polymerized by atom-transfer radical polymerization (ATRP) and spin-labeled with 4-amino-TEMPO at midchain as described in our previous article.²¹ The number-average molecular weight (M_n) and the molecular weight distribution (M_w/M_n , where M_w is the weight-average molecular weight) determined by gel permeation chromatography (GPC) were 24.9 kDa and 1.15, respectively.

2.3. Spin Probing. PS homopolymer ($M_n = 23.7$ kDa, $M_w/M_n = 1.10$) polymerized by ATRP and nitroxides were dissolved in toluene. The solution was casted onto a Teflon plate and dried in a hood for 1 day, and then the residual solvent in the sample film was completely removed in a vacuum at 388 K for 24 h. The typical concentration of the spin probe was 1×10^{-7} mol g⁻¹. For CHOL and BZONO, high concentrations were prepared (see Table 1).

Table 1. Dependence of $T_{g,ESR}$ and $T_{g,DSC}$ on Spin-Probe Concentration

spin probe	concentration (wt %)	concentration (mol g ⁻¹)	$T_{g,ESR}$ (K)	$T_{g,DSC}$ (K)
CHOL	~0	1.0×10^{-7}	374 ± 2	375 ± 2
CHOL	0.5	1.1×10^{-5}	374 ± 2	375 ± 2
CHOL	1.0	2.2×10^{-5}	372 ± 2	372 ± 2
CHOL	5.0	1.1×10^{-4}	370 ± 2	369 ± 2
BZONO	~0	1.0×10^{-7}	374 ± 2	375 ± 2
BZONO	5.0	1.8×10^{-4}	360 ± 2	360 ± 2

2.4. Preparation of PS/Silica Composite. For preparation of the composites, 0.95 or 0.98 g of silica powder dispersed in 1 mL of methyl ethyl ketone (MEK) was stirred and ultrasonicated for 1 h. Then, 0.05 or 0.02 g of PS containing 0.5 wt % CHOL was dissolved in 1 mL of MEK. These MEK solutions were mixed and vigorously stirred for 1 h. MEK was quickly blown off with a nitrogen stream under stirring in a hood. The samples were dried at 393 K for 24 h in a vacuum.

2.5. Measurements. Polymer samples for the ESR measurements were encapsulated in 5-mm-o.d. quartz tubes and sealed under a vacuum. Spectra were recorded with JEOL X-band (ca. 9 GHz) FA200 spectrometers with 100 kHz field modulation. The magnetic field and *g* tensor were calibrated with Mn²⁺. The temperature was controlled within ± 0.1 K. All samples were allowed to thermally equilibrate for at least 5 min after reaching the given temperature. For ESR spectral shape analyses, the samples were quenched to 173 K after being kept at 393 K for 15 min, and then the ESR measurements were performed stepwise from 173 to 463 or 433 K. The microwave power and modulation amplitude were kept small enough for each temperature to avoid broadening of the spectra. On the

other hand, for MPS measurements, the samples were quenched to 323 K after being kept at 393 K for 15 min, and then ESR measurements were performed stepwise from 323 to 398 K. The modulation amplitude was 0.2 mT, and the microwave power was 9–49 mW depending on the spin-probe reagent (described in detail in the next section). The magnetic field width, sweep time, and time constant were typically 15 mT, 60 s, and 0.03 s, respectively. The tuning parameters (phase and detector current) of the ESR spectrometer and sample position in the cavity were kept constant, and only temperature was varied for the MPS measurements.

Differential scanning calorimetry (DSC) was carried out using a Q10 differential scanning calorimeter manufactured by TA Instruments and calibrated with an indium standard. For the cooling of samples, a quench cooler accessory (TA Instruments) was used. The DSC cell was purged with dry nitrogen gas at a flow rate of 50 mL min⁻¹ during the measurements. Samples were heated from room temperature to ca. $T_g + 30$ K at a rate of 20 K min⁻¹, held for 5 min, cooled to ca. $T_g - 50$ K at a rate of 10 K min⁻¹, and heated to ca. $T_g + 30$ K at a rate of 10 K min⁻¹. The data were collected during the second heating process. The $T_{g,DSC}$ value was determined to be the midpoint, that is, the temperature corresponding to half of the endothermic shift including experimental uncertainties of ± 2 K. The $T_{g,DSC}$ value for PS was determined to be 375 K. Moreover, spin labeling and spin probing had no effect on $T_{g,DSC}$ at a concentration of 1×10^{-7} mol g⁻¹.

Gel permeation chromatography (GPC) was carried out with four polystyrene gel columns [Tosoh TSK gel GMH (bead size of 7 μ m), G4000H, G2000H, and G1000H (5 μ m)] connected to a Tosoh CCPE (Tosoh) pump and an ERC-7522 RI refractive index detector (ERMA Inc.) and with tetrahydrofuran as the eluent at 313 K in order to determine the weight- and number-average molecular weights of labeled PS samples. The column set was calibrated using standard PS (Tosoh) samples with narrow molecular weight distributions.

2.6. Determination of $T_{g,ESR}$ by the Microwave Power Saturation (MPS) Method. The principle of the MPS method was described in detail in our previous articles.^{17,18} This method determines the T_g value of spin-labeled and spin-probed polymers from the discontinuity in the slope of the plot of the natural logarithm of the saturation factor, S , versus the inverse of temperature, T^{-1} . The relative signal intensity, V_R , from the X-band ESR spectrometer is given by

$$V_R = \frac{\gamma H_1 (T_1 T_2)^{0.5}}{1 + \gamma^2 H_1^2 T_1 T_2} \quad (1)$$

where γ , H_1 , T_1 , and T_2 are the gyromagnetic ratio, microwave magnetic field, spin–lattice relaxation time, and spin–spin relaxation time, respectively.²² $\gamma^2 H_1^2 T_1 T_2$ is defined as the saturation factor, S , in this work. Without the saturation, V_R is proportional to H_1 because S is small enough to be ignored. In experiments, the V_R value obtained from double integration of a spectrum is proportional to the square root of the microwave power, $P^{0.5}$, because $H_1 \propto P^{0.5}$. On the other hand, deviations from the relationship of $V_R \propto P^{0.5}$ are observed when P is large because of an increase in S . This phenomenon is called microwave power saturation. When P is constant, S is determined from the ratio of the saturated V_R value, $V_{R,S}$, to the unsaturated value, $V_{R,US}$

$$\frac{V_{R,S}}{V_{R,US}} = \frac{1}{1 + S} \quad (2)$$

Therefore, the S is given by

$$S = \frac{V_{R,US}}{V_{R,S}} - 1 \quad (3)$$

In this work, the $V_{R,S}$ value at a certain power P of n mW was obtained from the double integration of the ESR spectrum measured at n mW, where n was 9, 16, 25, or 49. On the other hand, 0.02 mW was low enough to avoid saturation.¹⁸ Therefore, the $V_{R,US}$ value at n mW was calculated as

$$V_{R,US} = \left(\frac{n}{0.02} \right)^{1/2} V_{0.02\text{mW}} \quad (4)$$

where $V_{0.02\text{mW}}$ is the double integration value of the ESR spectrum measured at 0.02 mW. The inflection temperature in the slope of the temperature dependence of S was defined as $T_{g,ESR}$ (see Figure 4 below). As described in section 3.3, T_2 does not affect the value of $T_{g,ESR}$; the inflection of the temperature dependence of S at $T_{g,ESR}$ is due to the decrease in T_1 . We used microwave powers of 49, 25, 16, 16, and 9 mW for DBN, TEMPO, BZONO, CHOL, and the spin label, respectively. As described below, small spin probes had high mobility even in the glassy PS matrix; we found that higher P was appropriate for smaller spin probes because the microwave power saturation behavior was restrained by their high mobility. On the other hand, too much power decreases the signal-to-noise (S/N) ratio of the spectra and is inappropriate for accurate measurements. As a result, we chose the listed microwave power values for the respective samples. As shown in our previous work, the P value used for saturation does not affect the $T_{g,ESR}$ value.¹⁷ It should be noted that the absolute value of S determined by experiment is strongly influenced by many factors, such as the tuning parameters of the ESR spectrometer, the inserted sample position, and the shape of samples in the cavity; therefore, the direct comparison of absolute S values is hard without a precise control of the measurement conditions. However, we confirmed that the $T_{g,ESR}$ value was not influenced by such factors as long as the tuning parameters of the ESR spectrometer and the sample position were kept constant during the variable-temperature measurements.

3. RESULTS AND DISCUSSION

3.1. Dependence of Spin-Probe Size on $T_{g,ESR}$. The ESR spectral shape is dependent on the mobility of nitroxides; evaluations of the polymer dynamics through the ESR spectral shape of nitroxides doped as spin probes have been traditionally and widely performed.^{13,19,20,23} In this section, we show the effect of the spin-probe size on the mobility determined by ESR spectral shape analyses.

The chemical structures of the spin-labeled PS and nitroxides used as spin probes are shown in Figure 1. As an example, temperature-dependent ESR spectra for the PS spin-probed with TEMPO are shown in Figure 2. The ESR spectrum of nitroxides is dominated by the hyperfine interaction of the electron spin with the nuclear spin of the ¹⁴N nucleus ($I = 1$) and by g shifts due to spin–orbit coupling mainly in the 2p_z orbital of the lone pair on the oxygen nucleus. Usually, all orientations of nitroxides have the same probability; therefore, “powder” spectra are obtained when the rotational motion is frozen on the time scale of the experiment. However, the

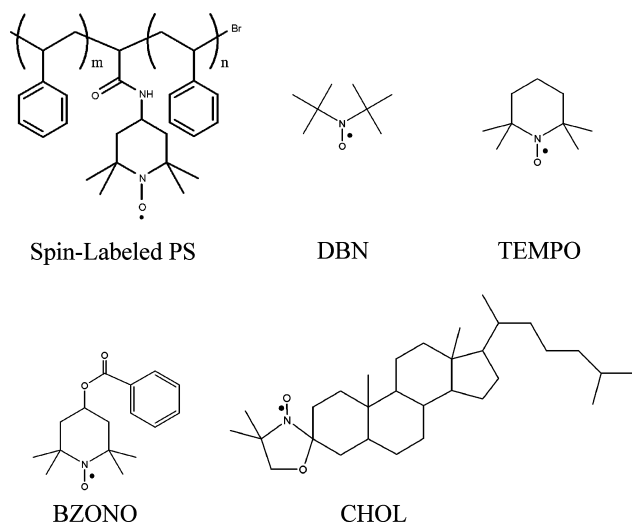


Figure 1. Chemical structures of spin-labeled PS and spin probes.

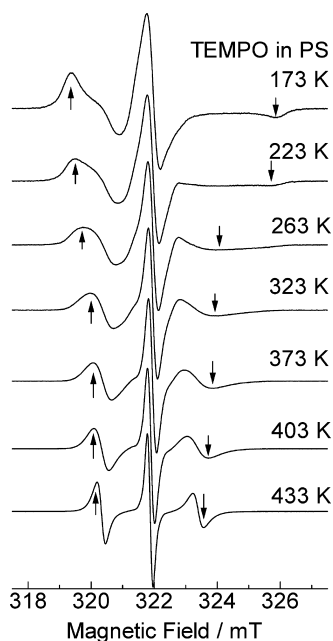


Figure 2. Temperature-dependent ESR spectra of spin-probed PS with TEMPO.

spectral anisotropy is averaged by the thermal rotational diffusion of nitroxides with increasing temperature, and the spectral shape becomes sharper. The mobility of nitroxides can be quantified by the rotational correlation time, τ_R , which is the time during which a molecule maintains its spatial orientation. The X-band ESR spectrum of nitroxide is sensitive to τ_R in the range of 10^{-11} – 10^{-7} s.¹⁴ On the other hand, when the τ_R is longer than 10^{-7} s or shorter than 10^{-11} s, the ESR spectrum is not sensitive to τ_R and little dynamics information can be deduced. τ_R is determined by spectral simulations based on proper models.^{24–26} In the present work, we simply compared the temperature dependences of extreme separations (ESs) for spin-probed and spin-labeled PSs. As shown in Figure 2, the ES indicated with arrows decreases with increasing temperature.

A plot of ES as a function of temperature is a visual indicator of the dynamics of nitroxides; this is a traditional but effective method for qualitatively comparing the dynamics in a series of materials.¹⁴ The ESs of each sample are plotted against

temperature in Figure 3. The ESs gradually narrow and steeply drop with an increase in temperature. In the present work, the

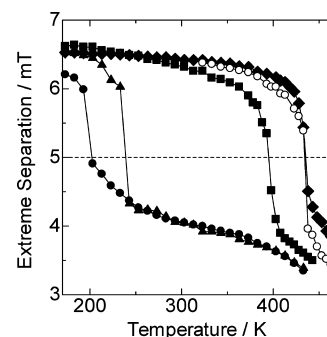


Figure 3. Temperature dependences of extreme separations (ESs) for spin-labeled PS (O) and spin-probed PS with DBN (●), TEMPO (▲), BZONO (■), and CHOL (◆). ES at 5 mT is shown with a dotted line.

temperature $T_{5\text{ mT}}$ at which the ES is 5 mT is defined as a reference temperature for the dynamics of nitroxides. The $T_{5\text{ mT}}$ values for spin-probed PS with DBN, TEMPO, BZONO, and CHOL and spin-labeled PS are 203, 239, 396, 435, and 435 K, respectively. Törmälä et al. suggested that the τ_R value corresponding to $T_{5\text{ mT}}$ lies between 4×10^{-9} and 10^{-8} s.¹⁹ The $T_{5\text{ mT}}$ value decreased with decreasing size of the spin probes; $T_{5\text{ mT}}$ for the largest spin probe, CHOL, was consistent with that for the spin label. This result is in good agreement with previous works where the dependence of $T_{5\text{ mT}}$ on the spin-probe size was evaluated for polyisobutylene¹⁹ and poly(methyl methacrylate).²⁰ The molecular weight dependences of the nitroxide on $T_{5\text{ mT}}$ were similar for these polymers even though the strength of the chemical interaction between the polymer and nitroxide was different for each case. This indicates that the nitroxide size is the main factor for the mobility of the nitroxide in polymer matrixes unless there is a strong chemical interaction, such as ionic and hydrogen bonds. Recently, we analyzed in detail the temperature dependence of the ESR spectral shape of the spin-labeled PS by computer simulation of experimental spectra and found the motion of the labeled nitroxide to be strongly coupled with that of PS segments due to the chemical linkage.²⁷ It is reasonably considered that molecular motion of the largest spin probe, CHOL, is also coupled with that of the surrounding PS segments. However, a reduction in motional coupling with decreasing spin-probe size was observed. Traditionally, the decoupling motion of small molecules in polymer matrixes is interpreted in terms of the concept of free volume.^{20,28–31} Specifically, when the size of the probe molecule is smaller than that of the free volume in the polymer matrix, a libration or wobbling motion of the probe molecules occur. In fact, Chernova et al. showed a strong correlation between the libration of nitroxide probes and the free volume size in glassy polymer matrixes.³² Recently, Nobukawa et al. studied the dynamics of low-mass molecules doped in PS in detail using dielectric spectroscopy.³³ For the small low-mass molecule 4-pentyl-4'-cyanobiphenyl (SCB), two dielectric relaxation modes (fast and slow modes) attributed to the full rotation motion and partial rotation motion, respectively, were found. They considered that the fast mode of SCB was governed by the size of the free space that induces the wobbling of SCB molecules and that the activation energy of the fast mode would be

determined by the local free volume size. On the other hand, for the larger molecule 4-pentyl-4'-cyanoterphenyl (SCT), the first mode was suppressed due to the large size of SCT, and only the slow mode (rotational mode) appeared. Unfortunately, line shape analysis of ESR spectra cannot distinguish the contributions of the two motional modes from the total mobility of the nitroxides. However, it is clearly shown that the motional coupling between the probe and PS segments decreases with decreasing spin-probe size.

3.2. Effect of Spin-Probe Size on $T_{g,ESR}$. In this section, the effects of the spin-probe size on the T_g value determined by the MPS method are discussed.

The natural logarithm of S for the spin-probed and spin-labeled PS is plotted against the inverse of T in Figure 4. The

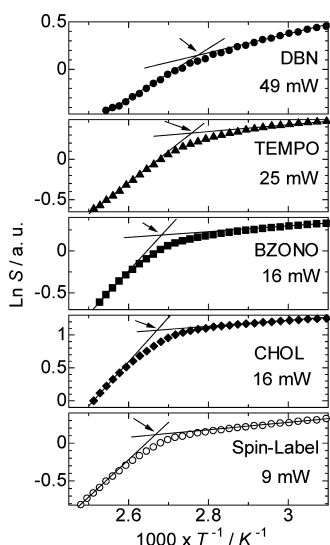


Figure 4. Temperature dependence of the saturation factor, S . $T_{g,ESR}$ is shown with an arrow. Applied microwave power is shown in the figure.

temperature at the inflection in the temperature dependence of S was defined as $T_{g,ESR}$. To verify the experimental uncertainty in $T_{g,ESR}$, the measurements were separately carried out more than three times for each sample. The $T_{g,ESR}$ values for spin-probed PS with DBN, TEMPO, BZONO and CHOL and spin-labeled PS are 360, 363, 374, 374, and 375 K, respectively. The experimental uncertainties are within 2 K. The $T_{g,ESR}$ values for the spin-labeled PS and spin-probed PS with BZONO and CHOL are in good agreement with the $T_{g,DSC}$ value, 375 K. This indicates that BZONO and CHOL are appropriate spin probes to detect the T_g value of PS using the MPS method; this is one of the most important conclusions in this work. It should be noted that no reduction in the T_g value of the PS by spin labeling or spin probing was confirmed by the DSC.

In Figure 5, the spin-probe size dependences for $T_{5 mT}$ and $T_{g,ESR}$ are compared. The $T_{5 mT}$ and $T_{g,ESR}$ values for spin-labeled PS are indicated in the figure with solid and broken lines, respectively. Both the $T_{g,ESR}$ and $T_{5 mT}$ values increased with increasing molecular weight of the spin probe; these values approached those for the spin-labeled PS. However, $T_{g,ESR}$ showed a much smaller size dependence than $T_{5 mT}$. As described in section 3.1, the ESR spectral shape is a function of the mobility of nitroxide, and the τ_R value corresponding to $T_{5 mT}$ lies between 4×10^{-9} and 10^{-8} s.¹⁹ Therefore, the τ_R value at $T_{g,ESR}$ must be shorter than 4×10^{-9} s for DBN and TEMPO, whereas it must be longer than 10^{-8} s for BZONO,

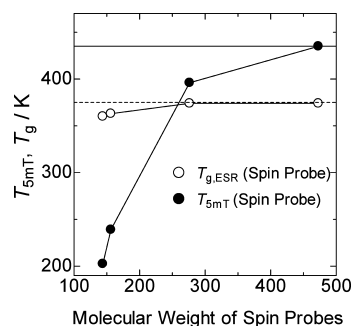


Figure 5. Plots of $T_{5 mT}$ and $T_{g,ESR}$ as a function of the molecular weight of the spin probes. $T_{5 mT}$ and $T_{g,ESR}$ for spin-labeled PS are shown with solid and dotted lines, respectively. $T_{g,ESR}$ for spin-labeled PS corresponds to $T_{g,DSC}$.

CHOL, and the spin label. That is, the τ_R value at $T_{g,ESR}$ is not constant for each nitroxide. The $T_{g,ESR}$ value reflects the change in the temperature dependence on the mobility of nitroxides induced by the glass transition of the PS segments surrounding nitroxides. Hence, $T_{g,ESR}$ exhibited a much smaller dependence on the spin-probe size than $T_{5 mT}$.

One might expect that the mobility of spin probes is directly enhanced by the segmental mobility of PS above T_g . However, the segmental mobility of PS must be too slow to enhance the mobility of nitroxides, especially for DBN and TEMPO, because the relaxation time of the polymer segments is about 100 s at T_g .³⁴ Therefore, it is reasonably considered that the mobility of small nitroxides is enhanced by the increase in the thermal expansion coefficient of the surrounding free volume.³⁵ Similarly, Nobukawa et al. recently observed a change in the temperature dependence of the fast mode (partial rotation mode) of 5CB in PS, poly(4-methylstyrene), and poly(4-*tert*-butylstyrene) around T_g , where the fast mode of 5CB was 10^3 – 10^6 times faster than the segmental motions of the matrix polymers.³⁶

For small spin probes, the $T_{g,ESR}$ values were significantly lower than the $T_{g,DSC}$ values. This result suggests that the small spin probes underwent the glass transition at temperatures lower than T_g of the matrix polymer. This phenomenon has been frequently reported, and scientific interest has been directed toward this mechanism. Savin et al. showed distinct two glass transitions in PS/solvent mixtures in DSC measurements and applied the concept of local effective concentrations for a qualitative interpretation of the two glass transitions.³⁷ This concept was proposed by Lodge and McLeish to explain the dynamic heterogeneity in miscible polymer blends.³⁸ They considered that the local effective concentration of one component must always be higher than the average concentration because of the self-concentration effect governed by chain connectivity. Savin et al. considered that the local length scale for small molecules is comparable to their molecular length; therefore, the local effective concentration of small molecules is always higher than the average concentration because of the high self-concentration effect. Inversely, the local effective concentration of small molecules approaches the average concentration as the molecular length increases, so the disagreement in the T_g values between for small molecule and polymer components disappears. More recently, Urakawa et al. pointed out that the rotational relaxation of small molecules doped in a PS matrix appeared near the calorimetric T_g value when the size of the small molecule became comparable to the Kuhn segmental size of the

PS.^{33,39,40} By assuming that the α (segmental) motion of PS should take place in the vicinity of T_g for mixtures with high PS contents, they concluded that the motion of small molecules and the α motion became cooperative for small molecules with sizes comparable to or larger than the Kuhn length of the polymers. These studies strongly suggest that the size of the spin probe is one of the most important factors for measuring the correct $T_{g,ESR}$ value to enhance the dynamic coupling between the spin probe and the polymer segments. We expect that CHOL and BZONO should be effective spin probes for most polymers. Additionally, strong chemical attractive forces between the spin probe and polymer segments, such as hydrogen and ionic bonds, also should be effective in enhancing the coupling.⁴¹

3.3. Concentration Effect of Spin Probe on $T_{g,ESR}$. High concentrations of spin probes improve the S/N ratio of the ESR spectrum; therefore, high concentrations are advantageous for accurate measurements of $T_{g,ESR}$. The effect of the spin-probe concentration on $T_{g,ESR}$ is examined in this section.

The temperature dependences of S for PSs containing 0.5, 1.0, and 5.0 wt % CHOL (1.1×10^{-5} , 2.2×10^{-5} , and 1.1×10^{-4} mol g⁻¹, respectively) are shown in Figure 6a, whereas that

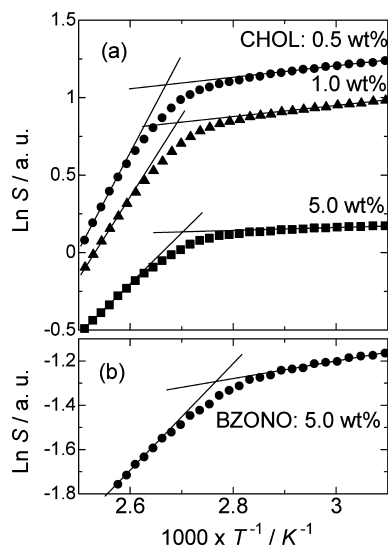


Figure 6. Temperature dependences of S for PS containing (a) 0.5, 1.0, and 5.0 wt % CHOL and (b) 5.0 wt % BZONO.

for PS containing 5.0 wt % BZONO (1.1×10^{-4} mol g⁻¹) is shown in Figure 6b. The $T_{g,ESR}$ and $T_{g,DSC}$ values for these samples are listed in Table 1. Both $T_{g,ESR}$ and $T_{g,DSC}$ decreased with increasing concentration of the spin probes because of the plasticizer effect of the excess spin probes; however, the $T_{g,ESR}$ and $T_{g,DSC}$ values were in good agreement for each concentration. There was a tendency for the absolute value of S to decrease with increasing spin-probe concentration. As described above, the absolute value of S determined by experiment is strongly influenced by many factors, such as the tuning parameters of the ESR spectrometer, the inserted sample position, and the shape of the samples in the cavity. Therefore, a direct comparison of the absolute S values makes no sense under normal conditions. Nevertheless, this tendency seemed to be beyond experimental errors. This behavior is reasonably considered to be due to the decrease in the spin–spin relaxation time, T_2 . That is, the excess concentration of spin probe increased the spin–spin interactions, and S was

reduced. This result clearly shows that the reduction of T_2 does not affect the value of $T_{g,ESR}$. As a conclusion, one can increase the spin-probe concentration to enhance the S/N ratio of the ESR spectrum unless the overall T_g value is decreased by blending of excess spin probes. This is practically important for applications of MPS to detect the T_g values of fractional components in multicomponent materials.

3.4. Detection of T_g in PS/Silica Composite. As a practical application of the MPS method, the detection of the $T_{g,ESR}$ value of the fractional PS component in PS/silica composites is considered in this section. The diameter of the silica particles was ca. 2 μ m. In the composite, the composition of PS was less than 5 wt %; therefore, the detection of the T_g value of the PS component is hard for conventional analytical methods, such as DSC, dilatometry, and dynamic mechanical analysis, to detect. Moreover, these samples are not adequate for modern optical T_g measurement methods^{5–7} because of their opacity and high scattering character.

CHOL was used as the spin probe, and the concentration for the PS component was 0.5 wt %. As shown in the previous section, the plasticizing effect of CHOL is low for this concentration. The PS/silica composite is denoted as COMP x , where x is the weight percentage of silica. The temperature dependences of S for PS, COMP95, and COMP98 are shown in Figure 7. The T_g value was clearly detected even for

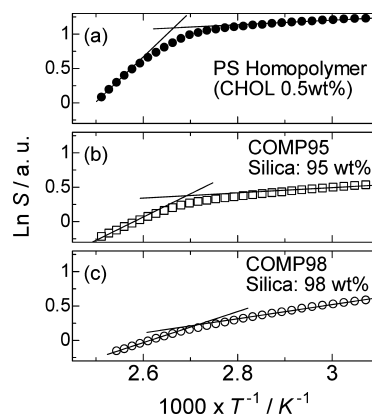


Figure 7. Temperature dependences of S for (a) PS containing 0.5 wt % CHOL and (b,c) PS/silica composite containing (b) 95 and (c) 98 wt % silica.

COMP98, and the change in slope of S in the vicinity of T_g became less pronounced with the increase in silica composition. This result indicates that the difference in the mobility of CHOL below and above T_g decreases with increasing silica composition. As described earlier, the mobility of the spin probe is strongly influenced by the thermal expansion of PS. Mizuno et al. measured the thermal expansion coefficient of PS/silica nanocomposites in the vicinity of T_g using capacitive scanning dilatometry.⁴² They reported a reduction of the thermal expansion coefficients of the PS component, especially above T_g , with increasing silica composition; the difference in the thermal expansion coefficients above and below T_g decreased upon the addition of silica. Our ESR results are considered to reflect the same phenomenon as observed in Mizuno et al.'s work.⁴²

The $T_{g,ESR}$ values for PS, COMP95, and COMP98 were determined to be 374 ± 2 , 371 ± 2 , and 358 ± 3 K, respectively. The decrease in $T_{g,ESR}$ with increasing composition

of silica was observed. According to many researcher's reports, the T_g values in polymer/silica (nano)composites show complicated behaviors; that is, they increase,^{8,9,43–46} decrease,^{8,9,42,45,47,48} or do not change^{8,9,42,45} depending on the strength of interactions at the polymer/solid interface, composition, morphology, and so on. Moreover, the increment and decrement in T_g also depend on these factors. For example, Bansal et al. showed that the T_g values for PS/silica nanocomposites were lower than that for the PS homopolymer and that the reduction of T_g was dependent on the average distance between silica particles.⁴⁸ In other words, the T_g value decreased with a decrease in the average distance between silica particles. They concluded that the mobility of PS near the particle surface might be enhanced by weak interactions between PS and silica particles and that this was the main cause for the reduction of T_g . Mizuno et al. also showed the reduction of T_g in the same nanocomposite as used in in Bansal et al.'s work by the capacitive scanning dilatometry measurement; however, the decrement was smaller than that in Bansal et al.'s work.⁴² Mizuno et al. concluded that the difference was due to the difference in the dispersity of silica. Bansal et al. additionally pointed out the importance of the polymer/particle wetting behavior on the T_g value in PS/silica nanocomposites.⁴⁵ In their work, silica nanoparticles grafted with dense PS brushes with a molecular weight of 110 kDa were blended with PS melts to form nanocomposites. When the molecular weight of the PS melts was less than 78 kDa, wetting of the particles was observed; concurrently, the T_g value of the nanocomposite increased. At higher molecular weight, the matrix did not wet the particles, and the T_g value decreased. On the other hand, some authors developed modern techniques to detect the local T_g value selectively at the polymer/solid interface.^{5–7} Ellison and Torkelson studied the distribution of T_g in PS thin films on silicon substrates using fluorescence intensity measurements. In this case, no change in T_g of a 12-nm layer at the PS/silicon interface in the PS film with a total thickness of ca. 280 nm was observed.⁷ Tanaka et al. recently showed an elevation of the T_g value at the PS/SiO_x interface by fluorescence lifetime measurements using evanescent wave excitation.^{5,6} When the detection depth was ca. 20 nm from the substrate surface, the increment of T_g was ca. 20 K. Furthermore, Porter and Blum showed an increase in T_g for PS adsorbed on silica using modulated differential scanning calorimetry.⁴⁴ They estimated the thickness of the adsorbed layer to be less than 2 nm. In our samples, the thickness of the PS component at the silica particle surface was not constant because the spacing between the silica particles was not uniform. Therefore, it is hard to discuss the decrement of $T_{g,ESR}$ quantitatively. However, we emphasize that the MPS method with spin probing is useful for selectively determining the T_g value of a fractional component in a multicomponent material.

4. CONCLUSIONS

An application of spin probing for the determination of $T_{g,ESR}$ by the MPS method of ESR spectroscopy was proposed as a simple and highly sensitive technique for fractional polymer components in multicomponent materials. The spin-probe size dependences of $T_{g,ESR}$ and $T_{5\text{ mT}}$ were first compared. The $T_{5\text{ mT}}$ values for spin-probed PS with DBN, TEMPO, BZONO, and CHOL and spin-labeled PS were determined to be 203, 239, 396, 435, and 435 K, respectively. On the other hand, the $T_{g,ESR}$ values for the same materials were 360, 363, 374, 374, and 375 K, respectively, within an experimental uncertainty of 2

K, whereas the $T_{g,DSC}$ value was 375 K for all samples. $T_{g,ESR}$ exhibited a much smaller spin-probe size dependence than $T_{5\text{ mT}}$ because $T_{g,ESR}$ reflects the change in the temperature dependence of the mobility of spin probes induced by the glass transition of the PS. The decrease in $T_{g,ESR}$ for small spin probes was considered to be due to the reduce in the motional coupling between small spin probes and PS segments. In addition, the effect of the spin-probe concentration on $T_{g,ESR}$ was evaluated. When the concentration of CHOL was more than 1.0 wt %, a decrease in the saturation factor, S , induced by shortening of the spin–spin relaxation time became obvious; $T_{g,ESR}$ decreased slightly with increasing weight fraction of CHOL because of the “plasticizer effect” of CHOL. However, the $T_{g,ESR}$ and $T_{g,DSC}$ values corresponded for each concentration. As a conclusion, large spin probes are appropriate for determining $T_{g,ESR}$ because of their strong motional coupling with polymer segments; the concentration of the spin probes does not affect the $T_{g,ESR}$ value unless the overall T_g value is reduced by blending of excess spin probes. Finally, the MPS method was applied for measurements of the T_g values in PS/silica composites containing more than 95 wt % silica. $T_{g,ESR}$ was clearly detected even for the composite containing 98 wt % silica, and a decrease in $T_{g,ESR}$ with increasing silica fraction was shown. We conclude that the MPS method with spin probing is a powerful and simple technique for selectively detecting the T_g values of fractional polymer components in multicomponent materials.

AUTHOR INFORMATION

Corresponding Author

*Tel./fax: +81-58-293-2565. E-mail: y_miwa@gifu-u.ac.jp.

Notes

The authors declare no competing financial interest.

REFERENCES

- (1) Strobl, G. R. *The Physics of Polymers*; Springer: Berlin, 1996; pp 237–256.
- (2) Sanchez, I., Ed. *Physics of Polymer Surfaces and Interfaces*; Butterworth-Heinemann: Boston, 1992; pp 1–262.
- (3) Kajiyama, T.; Tanaka, K.; Takahara, A. *Macromolecules* **1997**, *30*, 280–285.
- (4) Tanaka, K.; Takahara, A.; Kajiyama, T. *Macromolecules* **2000**, *33*, 7588–7593.
- (5) Tanaka, K.; Tsuchimura, Y.; Akabori, K.; Ito, F.; Nagamura, T. *Appl. Phys. Lett.* **2006**, *89*, 061916–061917.
- (6) Tanaka, K.; Tateishi, Y.; Okada, Y.; Nagamura, T.; Doi, M.; Morita, H. *J. Phys. Chem. B* **2009**, *113*, 4571–4577.
- (7) Ellison, C. J.; Torkelson, J. M. *Nat. Mater.* **2003**, *2*, 695–700.
- (8) Rittigstein, P.; Torkelson, J. M. *J. Polym. Sci. B: Polym. Phys.* **2006**, *44*, 2935–2943.
- (9) Rittigstein, P.; Priestley, R. D.; Broadbelt, L. J.; Torkelson, J. M. *Nat. Mater.* **2007**, *6*, 278–282.
- (10) Roth, C. B.; McNerny, K. L.; Jager, W. F.; Torkelson, J. M. *Macromolecules* **2007**, *40*, 2568–2574.
- (11) Roth, C. B.; Torkelson, J. M. *Macromolecules* **2007**, *40*, 3328–3336.
- (12) Mundra, M. K.; Donthu, S. K.; Dravid, V. P.; Torkelson, J. M. *Nano Lett.* **2007**, *7*, 713–718.
- (13) Jeschke, G. In *Advanced ESR Methods in Polymer Research*; Schlick, S., Ed.; Wiley: New York, 2006; Chapter 7, pp 165–195.
- (14) Jeschke, G.; Schlick, S. In *Advanced ESR Methods in Polymer Research*; Schlick, S., Ed.; Wiley: New York, 2006; Chapter 1, pp 3–24.
- (15) Andreozzi, L.; Giordano, M.; Leporini, D.; Martinelli, M.; Pardi, L. *Phys. Lett. A* **1991**, *160*, 309–314.

- (16) Sato, H.; Bottle, S. E.; Blinco, J. P.; Micallef, A. S.; Eaton, G. R.; Eaton, S. S. *J. Magn. Reson.* **2008**, *191*, 66–77.
- (17) Miwa, Y. *Macromolecules* **2009**, *42*, 6141–6146.
- (18) Miwa, Y.; Urakawa, O.; Doi, A.; Yamamoto, K.; Nobukawa, S. *J. Phys. Chem. B* **2012**, *116*, 1282–1288.
- (19) Törmälä, P.; Weber, G. *Polymer* **1978**, *19*, 1026–1030.
- (20) Tsay, F.-D.; Gupta, A. *J. Polym. Sci. B: Polym. Phys.* **1987**, *25*, 855–881.
- (21) Miwa, Y.; Tanase, T.; Yamamoto, K.; Sakaguchi, M.; Sakai, M.; Shimada, S. *Macromolecules* **2003**, *36*, 3235–3239.
- (22) Brezina, G. W.; Gelerinter, E. *J. Chem. Phys.* **1968**, *49*, 3293–3296.
- (23) Milner, W. G. In *Spin Labeling II. Theory and Applications*; Berliner, L. J., Ed.; Academic Press: New York, 1979; Chapter 4, pp 173–221.
- (24) Kivelson, D. *J. Chem. Phys.* **1960**, *33*, 1094–1106.
- (25) Freed, J. H. In *Spin Labeling: Theory and Applications*; Berliner, L. J., Ed.; Academic Press: New York, 1976; Chapter 3, pp 53–132.
- (26) Earle, K. A.; Budil, D. E. In *Advanced ESR Methods in Polymer Research*; Schlick, S., Ed.; Wiley: New York, 2006; Chapter 3, pp 53–83.
- (27) Miwa, Y.; Shimada, S.; Urakawa, O.; Nobukawa, S. *Macromolecules* **2010**, *43*, 7192–7199.
- (28) Bueche, F. *J. Chem. Phys.* **1962**, *36*, 2940–2946.
- (29) Kusumoto, N.; Sano, S.; Zaitzu, N.; Motozato, Y. *Polymer* **1976**, *17*, 448–454.
- (30) Vrentas, J. S.; Duda, J. L.; Ling, H.-C. *J. Polym. Sci. B: Polym. Phys.* **1985**, *23*, 275–288.
- (31) Vrentas, J. S.; Duda, J. L.; Ling, H.-C.; Hou, A.-C. *J. Polym. Sci. B: Polym. Phys.* **1985**, *23*, 289–304.
- (32) Chernova, D. A.; Vorobiev, A. K. H. *J. Polym. Sci. B: Polym. Phys.* **2009**, *47*, 107–120.
- (33) Nobukawa, S.; Urakawa, O.; Shikata, T.; Inoue, T. *Macromolecules* **2011**, *44*, 8324–8332.
- (34) Kauzmann, W. *Chem. Rev.* **1948**, *9*, 219–256.
- (35) Greiner, R.; Schwarzl, F. R. *Rheol. Acta* **1984**, *23*, 378–395.
- (36) Nobukawa, S. Ph.D. Thesis, Osaka University, Osaka, Japan, 2010.
- (37) Savin, D. A.; Larson, A. M.; Lodge, T. P. *J. Polym. Sci. B: Polym. Phys.* **2004**, *42*, 1155–1163.
- (38) Lodge, T. P.; McLeish, T. C. B. *Macromolecules* **2000**, *33*, 5278–5284.
- (39) Yoshizaki, K.; Urakawa, O.; Adachi, K. *Macromolecules* **2003**, *36*, 2349–2354.
- (40) Urakawa, O.; Ohta, E.; Hori, H.; Adachi, K. *J. Polym. Sci.: Polym. Phys.* **2006**, *44*, 967–974.
- (41) Hamada, K.; Iijima, T.; McGregor, R. *Macromolecules* **1987**, *20*, 215–220.
- (42) Mizuno, M.; Nakamura, K.; Konishi, T.; Fukao, K. *J. Non-Cryst. Solids* **2011**, *357*, 594–597.
- (43) Rong, J.; Yang, Z. *Macromol. Mater. Eng.* **2002**, *287*, 11–15.
- (44) Porter, C. E.; Blum, F. D. *Macromolecules* **2002**, *35*, 7448–7452.
- (45) Bansal, A.; Yang, H.; Li, C.; Benicewicz, B. C.; Kumar, S. K.; Schadler, L. S. *J. Polym. Sci. B: Polym. Phys.* **2006**, *44*, 2944–2950.
- (46) Moll, J.; Kumar, S. K. *Macromolecules* **2012**, *45*, 1131–1135.
- (47) Ash, B. J.; Siegel, R. W.; Schadler, L. S. *J. Polym. Sci. B: Polym. Phys.* **2004**, *42*, 4371–4383.
- (48) Bansal, A.; Yang, H.; Li, C.; Cho, K.; Benicewicz, B. C.; Kumar, S. K.; Schadler, L. S. *Nat. Mater.* **2005**, *4*, 693–698.